

## ARTICLE

# Contribution of cellulose synthesis, formation of fibrils and their entanglement to the self-flocculation of *Zymomonas mobilis*

Juan Xia<sup>1</sup> | Chen-Guang Liu<sup>1</sup> | Xin-Qing Zhao<sup>1</sup> | Yi Xiao<sup>2</sup> | Xiao-Xia Xia<sup>2</sup> |  
Feng-Wu Bai<sup>3</sup> 

<sup>1</sup>State Key Laboratory of Microbial Metabolism, Department of Bioengineering, Shanghai Jiao Tong University, Shanghai, China

<sup>2</sup>Joint International Research Laboratory of Metabolic and Developmental Sciences, Shanghai Jiao Tong University, Shanghai, China

<sup>3</sup>School of Life Science and Biotechnology, Shanghai Jiao Tong University, Shanghai, China

**Correspondence**

Xin-Qing Zhao, State Key Laboratory of Microbial Metabolism, Department of Bioengineering, Shanghai Jiao Tong University, 800 Dongchuan Rd., Shanghai, 200240, China.

Email: xqzhao@sjtu.edu.cn

Feng-Wu Bai, School of Life Science and Biotechnology, Shanghai Jiao Tong University, 800 Dongchuan Rd., Shanghai, 200240, China. Email: fwbai@sjtu.edu.cn

**Funding information**

National Natural Science Foundation of China, Grant/Award Number: 21536006

**Abstract**

Due to the unique Entner-Doudoroff pathway, *Zymomonas mobilis* has been acknowledged as a potential host to be engineered for biorefinery to produce biofuels and biobased chemicals. The self-flocculation of *Z. mobilis* can make the bacterial cells self-immobilized within bioreactors for high density to improve product productivities, and in the meantime enhance their tolerance to stresses, particularly product inhibition and the toxicity of byproducts released during the pretreatment of lignocellulosic biomass. In this work, we explored mechanism underlying such a phenotype with the self-flocculating strain ZM401 developed from the regular non-flocculating strain ZM4. Cellulase deflocculation and the restoration of the self-flocculating phenotype for the de-flocculated bacterial cells subjected to culture confirmed the essential role of cellulose biosynthesis in the self-flocculation of ZM401. Furthermore, the deactivation of both Type I and Type IV restriction-modification systems was performed for ZM4 and ZM401 to improve their transformation efficiencies. Comparative genome analysis detected the deletion of a thymine from ZMO1082 in ZM401, leading to a frame-shift mutation for the putative gene to be integrated into the neighboring downstream gene ZMO1083 encoding the catalytic subunit A of cellulose synthase, and consequently created a new gene to encode a larger transmembrane protein BcsA\_401 for more efficient synthesis of cellulose as well as the development of cellulose fibrils and their entanglement for the self-flocculation of the mutant. These speculations were confirmed by the morphological observation of the bacterial cells under scanning electron microscopy, the impact of the gene deletion on the self-flocculation of ZM401, and the restoration of the self-flocculating phenotype of ZM401Δ*bcsA* by the gene complementation. The progress will lay a foundation not only for fundamental research in deciphering molecular mechanisms underlying the self-flocculation of *Z. mobilis* and stress tolerance associated with the morphological change but also for technological innovations in engineering non-flocculating *Z. mobilis* and other bacterial species with the self-flocculating phenotype.

**KEYWORDS**

cellulose synthesis, fibrils formation and entanglement, frame-shift mutation, self-flocculation, *Zymomonas mobilis*

## 1 | INTRODUCTION

Compared to the Embden-Meyerhof-Parnas pathway in *Saccharomyces cerevisiae* with 2 mole ATP produced from 1 mole glucose metabolized, *Zymomonas mobilis* ferments glucose through the Entner-Doudoroff pathway with only 1 mole ATP produced, and consequently less biomass is accumulated for high ethanol yield (Bai, Anderson, & Moo-Young, 2008; Kalnenieks, 2006). But unfortunately, this species has never been used for ethanol production in the industry due to its narrow substrate spectrum. Ethanol production from lignocellulosic biomass provides opportunities for exploring the advantage of *Z. mobilis*, because only glucose is released from cellulose hydrolysis, and in the meantime this species can be engineered with xylose isomerase to convert xylose to xylulose directly without cofactor imbalance and xylitol accumulation that are intrinsic to *S. cerevisiae* engineered with xylose reductase and xylitol dehydrogenase for ethanol production from xylose (Jeffries, 2006; M. Zhang, Eddy, Deanda, Finkelstein, & Picataggio, 1995). In addition, *Z. mobilis* is also a potential host to be engineered for biorefinery to produce biobased chemicals such as 2, 3-butanediol (M. He et al., 2014; Yang, Fei et al., 2016; Yang, Mohagheghi et al. 2016).

The regular morphology of *Z. mobilis* is characterized by single cells measured at  $2\text{--}3 \times 1\text{--}2 \mu\text{m}$ , but the bacterial cells can self-flocculate to form flocs at a magnitude of hundreds of micrometers (Zhao et al., 2014). From the viewpoint of engineering, the self-flocculation of microbial cells presents advantages if the self-flocculating process is controlled properly without significant mass transfer limitation. On the one hand, cell flocs can be self-immobilized within bioreactors for high density to improve productivities of the bioreactors, particularly under continuous culture and fermentation conditions, which was highlighted in ethanol production by the self-flocculating *S. cerevisiae* (Zhao & Bai, 2009) and wastewater treatment in upflow anaerobic sludge blanket bioreactors using activated sludge granules developed by the self-flocculation of different microorganisms (Chong, Sen, Kayaalp, & Ang, 2012; Lim & Kim, 2014). On the other hand, enhanced tolerance to stresses such as ethanol produced during fermentation and acetic acid released from the hydrolysis of hemicelluloses during the pretreatment of lignocellulosic biomass was observed with the self-flocculating strains from *S. cerevisiae* and *Z. mobilis* (Xue, Zhao, & Bai, 2010; Zhao et al., 2014). We hypothesize that molecular mechanism underlying this phenomenon would be enhanced quorum sensing (QS) associated with the morphological change, particularly for *Z. mobilis*, because the self-flocculation of microbial cells characterized by cell-to-cell contact is the upper limit for high-density culture that is required for triggering QS (Papenfort & Bassler, 2016).

Although mechanism underlying the self-flocculation of *S. cerevisiae* has been elucidated for engineering other yeast strains with the phenotype (L. Y. He, Zhao, & Bai, 2012; Q. Li, Zhao, Chang, Zhang, & Bai, 2012), little has been done for the self-flocculation of *Z. mobilis*. *S. cerevisiae* is eukaryotic, and extracellular polymeric substances (EPSs) for its self-flocculation are glycoproteins (Halme, Bumgarner, Styles, & Fink, 2004; Soares, 2010; Verstrepen, Jansen, Lewitter, & Fink, 2005; Zhao & Bai, 2009), but *Z. mobilis* is prokaryotic, which lacks glycosylation function for proteins. Although lot of work has been done with EPSs in biofilms developed by pathogens and activated sludge for sewage treatment

(Flemming & Wingender, 2010; Liu et al., 2010), significant difference in morphologies among biofilms, activated sludge and the bacterial flocs indicates that EPSs flocculating *Z. mobilis* would be different, or these EPS components might interact through different mechanism. Moreover, in addition, most biofilms and all activated sludge are formed by mixed organisms through mutualistic symbiosis among different species (Flemming et al., 2016; Ju & Zhang, 2015), which are also different from the self-flocculation of *Z. mobilis* under pure culture conditions. In addition, *Z. mobilis* has evolved with restriction-modification (R-M) systems such as Type I and Type IV, which not only protect it from the invasion of foreign DNA but also impede genetic manipulations on the species. Although deactivation of the single R-M system was attempted (Kerr, Jeon, Svenson, Rogers, & Neilan, 2011), the effort is still needed for developing deactivated mutants to transform *Z. mobilis* more efficiently for fundamental research and technological innovations.

In this work, the contribution of cellulose biosynthesis to the self-flocculation of *Z. mobilis* was studied, and mutants with the dual R-M systems deactivated were developed. The progress will lay a foundation for further fundamental research in deciphering mechanism underlying the self-flocculation of *Z. mobilis* and stress tolerance associated with the morphological change as well as technological innovations for engineering non-flocculating *Z. mobilis* and other bacterial strains with desired self-flocculating phenotypes.

## 2 | MATERIALS AND METHODS

### 2.1 | Strains, media, and enzymes

*Escherichia coli* DH5 $\alpha$  and *E. coli* JM110 was used for the propagation of plasmids carrying genes with and without methylation, respectively, to check the impact of the deactivation of the R-M system(s) on the transformation of *Z. mobilis*, which were cultured with the Luria-Bertani medium composed of 10 g/L tryptone, 5 g/L yeast extract and 10 g/L NaCl in flasks at 37°C and 200 rpm. *Z. mobilis* strains, the non-flocculating ZM4, and self-flocculating ZM401, were purchased from American Type Culture Collection (ATCC), which were cultured in a rich medium composed of 10 g/L yeast extract, 20 g/L glucose, and 2 g/L KH<sub>2</sub>PO<sub>4</sub> at 30°C and 150 rpm. When 20  $\mu\text{g/ml}$  tetracycline or 5% sucrose was supplemented, the rich medium was used for positive- and counter-section (Hmelo et al., 2015). All strains used in this study are given in Table 1.

Enzymatic hydrolysis was designed to identify polysaccharides in the EPSs for the self-flocculation of ZM401, and enzymes that specially hydrolyze different glycosidic bonds were selected, including  $\alpha$ -amylase and glucoamylase donated by COFCO Nutrition and Health Research Institute, China to hydrolyze  $\alpha$ -glycosidic bonds as well as cellulases (Novozymes), endo- $\beta$ -glucanase (Sigma), cellobiase and  $\beta$ -glucosidase (Novozymes) to hydrolyze  $\beta$ -(1 $\rightarrow$ 4) linked glycosidic bonds.

### 2.2 | Calcofluor-white staining assay

Calcofluor-white staining was used to qualitatively evaluate cellulose synthesized by *Z. mobilis* (Cowles, Willis, Engel, Jones, & Barak, 2015).

**TABLE 1** Strains used in this study

Strains	Description	References
<i>E. coli</i> DH5 $\alpha$	<i>lacZ</i> $\Delta$ M15, <i>recA</i> 1	
<i>E. coli</i> JM110	<i>rpsL</i> , <i>dam</i> <sup>-</sup> , <i>dcm</i> <sup>-</sup>	
<i>Z. mobilis</i> ZM4	ATCC31821	
<i>Z. mobilis</i> ZM401	ATCC31822	
ZM401 $\Delta$ <i>bcsA</i>	ZM401 with <i>bcsA</i> deleted	This study
ZM401 $\Delta$ <i>bcsA</i> / <i>bcsA</i> <sub>ZM4</sub>	ZM401 $\Delta$ <i>bcsA</i> complemented with <i>bcsA</i> from ZM4	This study
ZM401 $\Delta$ <i>bcsA</i> / <i>bcsA</i> <sub>401</sub>	ZM401 $\Delta$ <i>bcsA</i> complemented with <i>bcsA</i> <sub>401</sub> from ZM401	This study
ZM401 $\Delta$ <i>bcsA</i> / <i>bcsA</i> <sub>401</sub> <sup>R575A</sup>	ZM401 $\Delta$ <i>bcsA</i> complemented with <i>bcsA</i> <sub>401</sub> <sup>R575A</sup>	This study
ZM4m	ZM4 deleted with ZMO0028 and ZMO1933	This study
ZM401m	ZM401 deleted with ZMO0028 and ZMO1933	This study

The fluorescent dye was supplemented at 20  $\mu$ g/ml into 1 ml culture with OD<sub>600</sub> adjusted to 1.0, and the mixture was incubated at room temperature under dark conditions for 1 hr, which was then centrifuged at 12,000g for 1 min to collect cell pellets, washed twice with deionized (DI) water and re-suspended to 1 ml by DI water for fluorescence analysis. The fluorescence density was measured by ENSPIRE 2300 (PerkinElmer, Waltham, MA) at an excitation of 360 nm and an emission of 460 nm.

### 2.3 | Electron microscopy characterization

The morphology of *Z. mobilis* was observed under scanning electron microscopy (SEM). Samples were prepared as previously reported with

minor modifications (Gu, Zhang, & Bao, 2015). Briefly, cells were collected, washed with phosphate buffer solution (PBS), and then fixed with 2.5% glutaraldehyde for 4 hr. After washing three times with PBS, the cells were sequentially dehydrated by 50%, 70%, 90%, and 100% ethanol for 15 min, which was then subjected to critical point drying and coated with gold for SEM observation using Hitachi S-3400N.

### 2.4 | Characterization of the self-flocculation of *Z. mobilis*

The flocculating efficiency of *Z. mobilis* was quantified by the method reported previously with modifications on the de-flocculation of the bacterial flocs (Palha, Lopes, & Pereira, 1997). Simply, test tubes, each with 5 ml culture, were shaken vigorously for homogenous suspension, and then rested for 5 min. Suspension of 200  $\mu$ l was sampled from the upper section to measure OD<sub>600</sub> to quantify the non-flocculating cells ( $C_f$ ). Based on the previous study on the de-flocculation of ZM401 by cellulase, cellulase (Novozymes) at designated dosages was supplemented into the culture, which was incubated at 50°C for complete de-flocculation of the bacterial flocs to measure the concentration of total cells ( $C_t$ ). The flocculating efficiency (R%) of *Z. mobilis* was evaluated by the calculation:  $R\% = (1 - C_f/C_t) \times 100$ .

### 2.5 | Genetic manipulations

Plasmids and primers used in this study are given in Table 2 and Table 3. Gene deletion was performed by homologous recombination with the suicide vector pEX18Tc bearing tetracycline selection marker (*tetA*) and sucrose counter-selection marker (*sacB*, which are illustrated schematically in Figure 1a and b, respectively). Briefly, 500–1,000 bp fragments flanking gene to be deleted were amplified, and fused by overlap extension polymerase chain reactions (SOE-PCR). The final PCR products were purified, and digested with restriction enzymes for cloning into the suicide plasmid to develop recombinant plasmids, which

**TABLE 2** Plasmids used in this study

Plasmids	Description	References
pEX18Tc	Tc <sup>R</sup> , oriT <sup>+</sup> , <i>sacB</i> <sup>+</sup> , gene replacement vector with MCS from pUC18	Hoang et al. (1998)
pHW20a	Tc <sup>R</sup> , <i>mob</i> (RP4), <i>mob</i> (RSF1010), <i>lacZ</i> $\alpha$ , MCS and <i>oriV</i>	Dong et al. (2011)
pEX18Tc:: $\Delta$ 1933	Fragment flanking ZMO1933 of ZM4 ligated into pEX18Tc	This study
pEX18Tc:: $\Delta$ 0028	Fragment flanking ZMO0028 of ZM4 ligated into pEX18Tc	This study
pEX18Tc:: $\Delta$ <i>bcsA</i>	Fragment flanking <i>bcsA</i> of ZM401 ligated into pEX18Tc	This study
pHW20a:: <i>bcsA</i>	<i>bcsA</i> from ZM4 ligated into pHW20a with the <i>pdC</i> <sup>Zm</sup> promoter	This study
pHW20a:: <i>bcsA</i> <sub>401</sub>	<i>bcsA</i> <sub>401</sub> from ZM401 ligated into pHW20a with the <i>pdC</i> <sup>Zm</sup> promoter	This study
pHW20a:: <i>bcsA</i> <sub>401</sub> <sup>R575A</sup>	Mutated <i>bcsA</i> <sub>401</sub> from ZM401 ligated into pHW20a with the <i>pdC</i> <sup>Zm</sup> promoter	This study

**TABLE 3** Primers used in this study

Primers	Sequences	Description
Δ0028-up-F	<u>CGGAATTCGGCGGTATTTTCTCCAGTC</u>	Deletion of ZMO0028 in ZM4 or ZM401
Δ0028-up-R	<u>GAAATCCAAATCAACCCGTTTGCTGGGAACCGCCATTATCG</u>	
Δ0028-down-F	<u>CGATAATGGCGGTTCCCAGCAAACGGGTTGATTGGATTTC</u>	
Δ0028-down-R	<u>CGGGATCCAACGGCTGACCAAAACTATCC</u>	
Δ1933-up-F	<u>ACGGGATCCTCGGCTTCGACGTCCTTATG</u>	Deletion of ZMO1933 in ZM4 or ZM401
Δ1933-up-R	<u>GGTCAAGGTAAGCCATGGCGCAGATCGCTTAGGCGATCTTG</u>	
Δ1933-down-F	<u>CAAGATCGCCTAAGCGATCTGCGCCATGGCTTACCTTGACC</u>	
Δ1933-down-R	<u>TAAGTGCAGGGTTGCAGCCGTCGTAGAAC</u>	
Δ1083-up-F	<u>CGGAATTCGTCTGTCGAAACGATGGATG</u>	Deletion of <i>bcsA</i> <sub>401</sub> in ZM401
Δ1083-up-R	<u>GATGCGATGGTTGAAACAGGATAGAGGCAAATGGCTTGG</u>	
Δ1083-down-F	<u>CCAAGCCATTTTGCTCTATCCTGTTTCAACCATCGCATC</u>	
Δ1083-down-R	<u>ACGGGATCCCAAATCTGTCAAAGAAAGGC</u>	
<i>Ppdc</i> -F	<u>CGGCCAGTGAATTCGAGCTCTTATCGCTCATGATCGCGGC</u>	Amplification of the pyruvate decarboxylase promoter
<i>Ppdc</i> -R	<u>TGCTTACTCCATATATTCAAAC</u>	
1082-F	<u>GTTTTGAATATATGGAGTAAGCAATGCTTCATAAAAGCCGTAT</u>	Amplification of <i>bcsA</i> <sub>401</sub>
1083-F	<u>CTTAATAAGTTAGGAGAATAAACATGGGATTGACGCTGCTGAT</u>	Amplification of ZMO1083
1083-R	<u>ATTACGCCAAGCTTGCATGCTCATTCTTTACTGCCCCCT</u>	
<i>bcsA</i> <sub>401</sub> <sup>R575A</sup> -up-R	<u>GCGCATCTGCCTACTTTCATGGGCGA</u>	Substitution of the 575th Arginine of <i>bcsA</i> <sub>401</sub> by Alanine
<i>bcsA</i> <sub>401</sub> <sup>R575A</sup> -down-F	<u>TCGCCATGAAAGTAGGCAGATCGCCAATAC</u>	

Note. The underlines indicated homologous sequences for fusion into adjacent fragments, and the black bold character indicated restriction enzymes sites.

were propagated in *E. coli* DH5 $\alpha$ , and confirmed by sequencing. Due to the R-M systems in *Z. mobilis*, the confirmed plasmids were further transformed into *E. coli* JM110 for demethylation and more efficient transformation into ZM4 and ZM401 through electroporation by the Bio-Rad Gene Pulser with 0.1 cm gap cuvettes operated at 16 kV/cm, 200  $\Omega$  and 25  $\mu$ F. The positive selection was performed using the rich medium supplemented with tetracycline after the first crossover recombination. Then, the second crossover recombination was performed, and a mutant with the gene deleted was selected through the counter-selection using the rich medium supplemented with sucrose (X. Li, Thomason, Sawitzke, Costantino, & Court, 2013), which was confirmed by PCR. For gene overexpression/complementation, promoters and target genes were amplified separately by PCR. The recombinant plasmids were constructed through inserting promoters and target genes into the shuttle vector pHW20a (Figure 1c) by seamless cloning (Dong, Bao, Ryu, & Zhong, 2011), which were propagated in *E. coli* DH5 $\alpha$  and *E. coli* JM110 and confirmed by sequencing. The transformation procedures of these plasmids were the same as that applied with the plasmids used for the gene deletion.

## 2.6 | RNA extraction and transcription analysis

Cells were harvested at the exponential growth stage. Total RNA was extracted using the Spin Column Bacterial total RNA Purification Kit (Sango, Shanghai, China) according to the manufacturer's instructions.

One microgram RNA was used as a template to synthesize cDNA using the PrimeScript™ RT reagent cDNA Kit (Takara, Japan). Gene transcription was quantified by quantitative PCR (qPCR) with the CFX System (Biorad, Hercules, CA), and the transcription of 16s RNA was used as the reference for normalization (K. Zhang et al., 2015).

## 2.7 | Evaluation of cell growth and ethanol fermentation

Stock culture was transferred from agar plates using an inoculating loop, and inoculated into 250 ml Erlenmeyer flasks containing 100 ml rich medium for seed culture, which was performed overnight in a shaker at 30°C and 150 rpm to exponential phase for inoculation at 20% (v/v) into 250 ml Erlenmeyer flasks containing 100 ml medium composed of 100 g/L glucose, 10 g/L yeast extract, and 2 g/L KH<sub>2</sub>PO<sub>4</sub>. The culture and ethanol fermentation was also performed in shakers at 30°C and 150 rpm, and time-courses were monitored by sampling at designated intervals.

Cell growth was characterized by OD<sub>600</sub>. For the self-flocculating *Z. mobilis* strains, the de-flocculation of the bacterial flocs by cellulase was performed before the measurement of OD<sub>600</sub>. After the measurement of OD<sub>600</sub>, the samples were centrifuged at 12,000g for 1 min to remove cells, and the supernatant was filtered by 0.22  $\mu$ m membrane for the analysis of ethanol and residual glucose using HPLC (Waters e2695 with a Bio-Rad Aminex HPX-87H organic

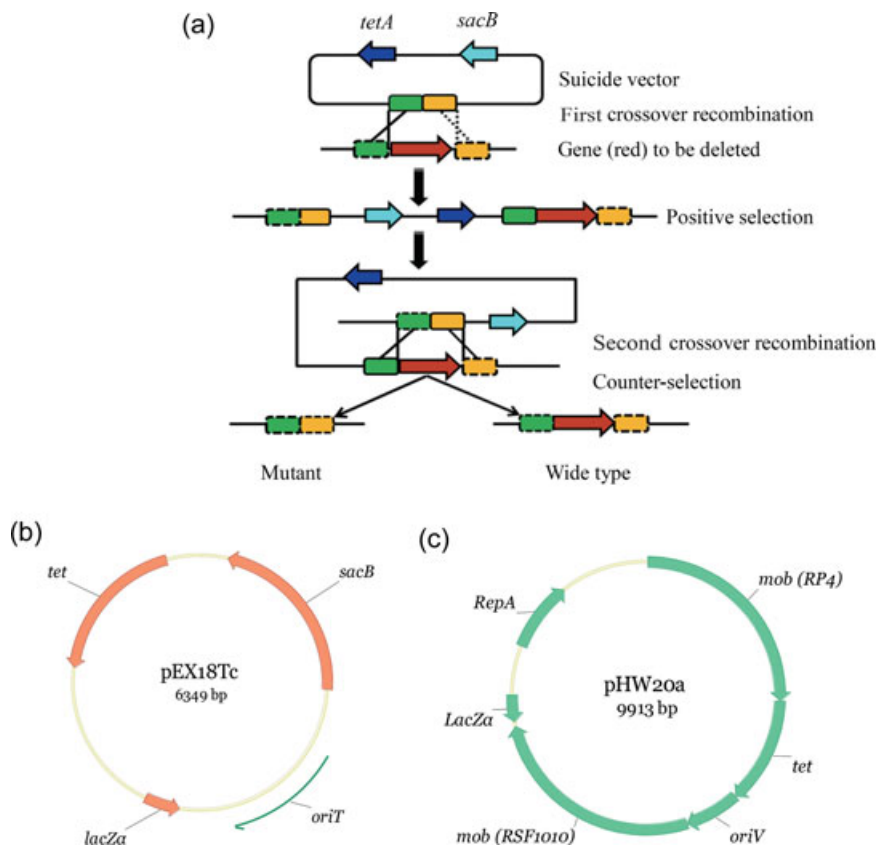


**FIGURE 1** Strategies for homologous recombination (a) and development of vectors for gene deletion (b) and expression/complementation (c) [Color figure can be viewed at [wileyonlinelibrary.com](http://wileyonlinelibrary.com)]

acids column and refractive index detector 2414). The oven temperature was set at 65°C and 4 mM H<sub>2</sub>SO<sub>4</sub> (0.6 ml/min) was used as the mobile phase.

### 3 | RESULTS AND DISCUSSION

#### 3.1 | Identification of the role of cellulose in the self-flocculation of ZM401

Previous studies assumed that cellulose could be the major EPS for the self-flocculation of ZM401 (Jeon, Xun, Su, & Rogers, 2012). Moreover, protease treatment could not de-flocculate the bacterial flocs, which not only ruled out the possibility for proteins including flagella to flocculate the bacterial cells but also indicated the role of polysaccharides in the self-flocculation of the bacterial cells. Initially, we tried to characterize the cellulose component directly in the EPS extracted from the self-flocculated bacterial cells, but unfortunately, we were not successful due to the low EPS content for extraction. Therefore, we had to look for alternatives and turned to enzymatic hydrolysis of the EPS for indirect evidence to confirm the role of cellulose in the self-flocculation of ZM401.

The impact on the self-flocculation of ZM401 when treated by different carbohydrate hydrolytic enzymes is shown in Figure 2a. Both  $\alpha$ -amylase and glucoamylase could not de-flocculate the flocs,

which ruled out the possibility for the bacterial cells to be flocculated through polysaccharides linked by  $\alpha$ -glycosidic bonds either starch or dextrin, particularly dextrin that is glutinous. Endo- $\beta$ -glucanase that specifically hydrolyzes  $\beta$ -(1→4) linked glycosidic bonds into cello-dextrin deflocculated the bacterial flocs significantly but not completely as that observed in the treatment by cellulases. Both cellobiase and  $\beta$ -glucosidase alone could not de-flocculate the bacterial flocs, but when the two enzymes were supplemented sequentially into the sample treated by endo- $\beta$ -glucanase, the complete de-flocculation of ZM401 occurred. These experiments supported our conclusion that cellulose rather than other polysaccharides flocculates the bacterial cells.

Figure 2b further quantifies the de-flocculation of ZM401 by cellulases supplemented at the dosages of 0.30 U/ml and 0.03 U/ml, respectively, into the suspension adjusted to the same cell density of OD<sub>600</sub> = 2.0 detected after the flocs were de-flocculated completely. As can be seen, the bacterial flocs were de-flocculated effectively by cellulase, particularly when cellulase was supplemented at the higher dosage of 0.30 U/ml, and a complete de-flocculation was observed within 10 min. Under the lower cellulase dosage of 0.03 U/ml, the incubation time was extended to 30 min for a complete de-flocculation. From the viewpoint of the intrinsic kinetics of enzymatic catalysis and mass transfer associated with the heterologous reaction, the reasons for this phenomenon might be: (a) lower

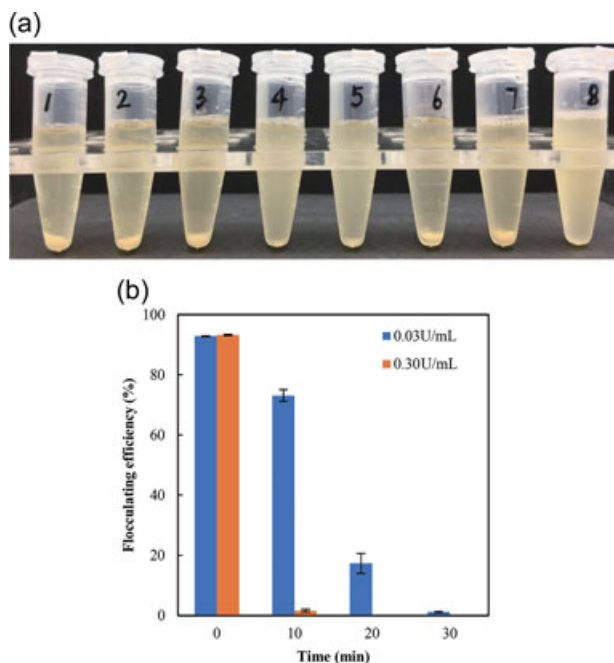


**FIGURE 2** Impact of enzymatic treatment on the self-flocculation of ZM401. (a) Incubated at 84°C without supplementation of any enzyme as the control (1), and treatment of 2 hr at 84°C by  $\alpha$ -amylase (2), 60°C by glucoamylase (3), and 50°C by cellulases (4), endo- $\beta$ -1, 4-glucoanase (5), cellobiase (6),  $\beta$ -glucosidase (7), and endo- $\beta$ -1,4-glucoanase+cellobiase+ $\beta$ -glucosidase (8). All enzymes were supplemented with overdosages. De-flocculation of ZM401 by cellulase supplemented at 0.03 U/ml and 0.30 U/ml, respectively (b). The initial cell density was adjusted to  $OD_{600} \cong 2.0$  which was measured after the bacterial flocs were completely de-flocculated. The enzymatic hydrolysis was performed at 50°C [Color figure can be viewed at [wileyonlinelibrary.com](http://wileyonlinelibrary.com)]

maximal rate associated with the lower uploading of cellulase, and (b) lower driving force in mass transfer for cellulase to diffuse into the inside of the bacterial flocs.

On the other hand, the de-flocculated bacterial cells restored their self-flocculating phenotype when cellulase was removed by decanting the supernatant after the suspension was centrifuged, and the cell pellets were re-suspended in the fresh medium and cultured at 30°C for cellulose regeneration, because flocculating efficiency as high as 90% was detected after culture for 90 min, but the increase in cell numbers characterized by  $OD_{600}$  was only 43.5% (Figure 3a), indicating that contribution to the self-flocculating phenotype was mainly from cellulose regeneration by the de-flocculated bacterial cells rather than their propagation. Such speculation was further confirmed by the morphological difference observed in the SEM images, because smooth surfaces were observed for the bacterial cells subjected to cellulase treatment, but cellulose fibrils were observed on the surfaces of ZM401 and the de-flocculated bacterial cells subjected to the culture (Figure 3b–d). Although cellulose has been reported as one of the architectural elements of bacterial biofilms (Flemming et al., 2016; Serra, Richter, & Hengge, 2013), its role in the self-flocculation of *Z. mobilis* is significantly different, because the entanglement of

cellulose fibrils was clearly observed in the SEM image. These results not only confirmed the role of extracellular cellulose fibrils and their entanglement in the self-flocculation of ZM401 but also provided a strategy for restoring the self-flocculating phenotype once the bacterial flocs are de-flocculated by cellulase.

### 3.2 | Deactivation of the R-M systems

*Z. mobilis* has evolved with R-M systems for defense against invasion of foreign DNA, which should be deactivated properly for efficient genetic manipulations. However, physiological properties and metabolic performance should not be affected substantially so that the R-M system deactivated mutants are suitable for fundamental research and technological innovations.

Transformation efficiencies of both methylated and unmethylated plasmids were increased when ZMO1933 and ZMO0028 related to Type I and Type IV R-M systems in *Z. mobilis* ZM4 were knocked out separately (Kerr et al., 2011), but the researchers could not obtain mutants with both I and IV R-M systems deactivated due to the lack of suitable selective markers. Herewith, we deactivated both Type I and Type IV R-M systems in ZM4 and ZM401 to further improve their transformation efficiencies (Figure 4a,b), which were examined by the transformation of the shuttle vectors pHW20a and pHW20a (Dam<sup>-</sup>, Dcm<sup>-</sup>). The growth and ethanol fermentation performance of the mutants ZM4m and ZM401m are shown in Figure 4c,d. In addition, we compared the transformation efficiency of ZM4 with both the R-M systems deactivated and the deactivation of the R-M system either Type I or Type IV.

While almost no transformant was obtained when the wide-type ZM4 and ZM401 were transformed by pHW20a amplified in *E. coli* DH5 $\alpha$ , the transformation efficiencies of  $2.1 \times 10^4/\mu\text{g(DNA)}$  and  $1.2 \times 10^4/\mu\text{g(DNA)}$  were achieved, respectively, for the mutants of ZM4 and ZM401 with both the R-M systems deactivated. When the plasmid was amplified in *E. coli* JM110, the transformation efficiencies were  $8.0 \times 10^2/\mu\text{g(DNA)}$  and  $3.3 \times 10^2/\mu\text{g(DNA)}$  for the wide-type ZM4 and ZM401, but were increased drastically to  $2.4 \times 10^4/\mu\text{g(DNA)}$  and  $1.5 \times 10^4/\mu\text{g(DNA)}$  after the R-M systems were deactivated. Moreover, higher transformation efficiency was observed for ZM4 with both the R-M systems deactivated compared to the deactivation of either of them. No significant impact was observed in cell growth, glucose consumption and ethanol production between the wide-type strains and their mutants with the R-M systems deactivated. On the other hand, the deactivation of the R-M systems in ZM401 did not disrupt its self-flocculation phenotype. Therefore, the mutants with both the R-M systems deactivated would benefit to experimental studies of molecular mechanism underlying the self-flocculation of ZM401 and other genetic modifications on *Z. mobilis*.

### 3.3 | Mutations in genes responsible for cellulose synthesis in ZM401

The comparative transcriptome analysis between ZM401 and ZM4 revealed differential expression of genes in ZM401: the expression of

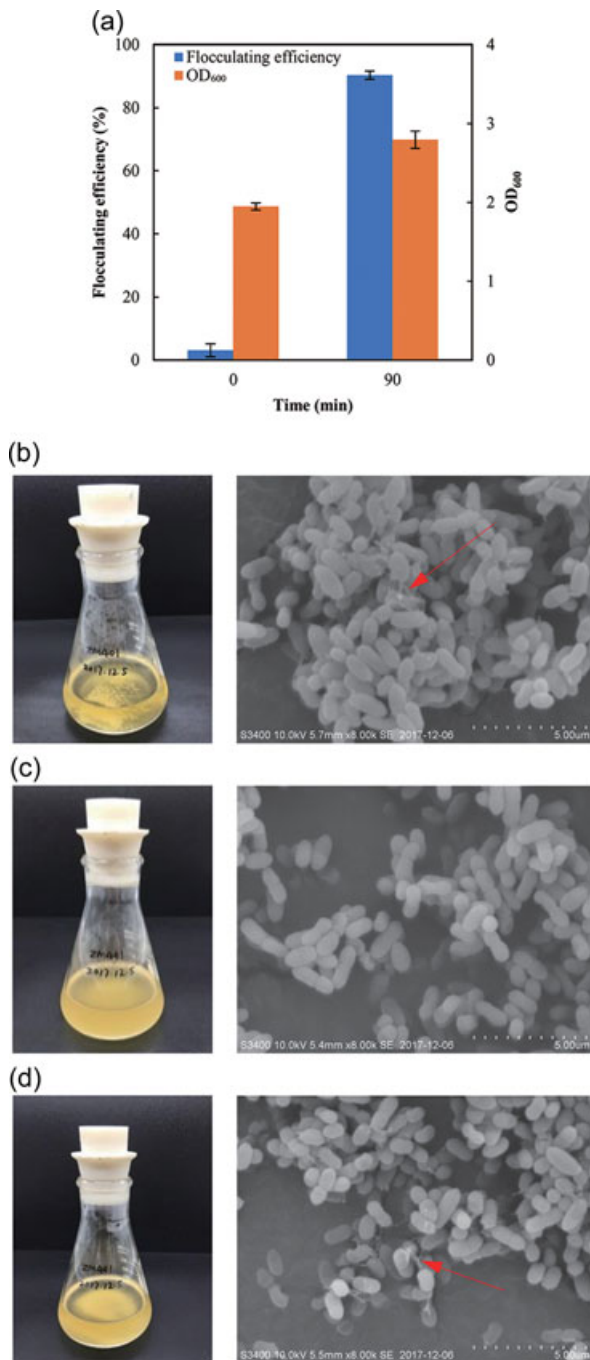


**FIGURE 3** Restoration of the self-flocculating phenotype of ZM401 cells subjected to cellulase treatment (a) and morphological differences observed by SEM for ZM401 cells (b), ZM401 cells subjected to cellulase treatment (c) and the culture of de-flocculated bacterial cells (d). SEM: scanning electron microscopy, and the red arrows indicate the entanglement of cellulose fibrils [Color figure can be viewed at [wileyonlinelibrary.com](http://wileyonlinelibrary.com)]

ZMO1083 and ZMO1084 that might relate to cellulose biosynthesis was upregulated, but the expression of ZMO0608, ZMO0611, ZMO0612, ZMO0613 and ZMO0614 for the synthesis of flagella-related proteins was downregulated, indicating that enhanced cellulose production and reduced flagella activities could facilitate the self-flocculation of *Z. mobilis* (Jeon et al., 2012). Cellulose is

different from other polysaccharides that are sticky to glue bacterial cells together and also makes them adhered to surfaces of supporting materials for biofilms formation (Limoli, Jones, & Wozniak, 2015), which flocculated ZM401 through the entanglement of cellulose fibrils (Figure 3b,d). Such a cellulose matrix is porous for more efficient mass transfer, which was validated experimentally by our previous studies on the growth and ethanol fermentation performance of ZM401 (Zhao et al., 2014). On the other hand, the potential reduction in the synthesis of flagellum proteins could not be the root reason for the self-flocculation of ZM401, because the function of flagella is mainly for bacterial cells to swim rather than glue or entangle together for their self-flocculation.

We sequenced the genome of ZM401 (Zhao, Bai, Zhao, Yang, & Bai, 2012), and compared to that of ZM4 previously reported (Seo et al., 2005; Yang et al., 2009). A deletion of nucleotide (Thymine) in ZMO1082 was detected in ZM401, which consequently created a frame-shift mutation as illustrated in Figure 5a. In ZM4, ZMO1082 is a putative gene, which is predicted to encode a peptide composed of 67 amino acid residues with unknown functions. It is less likely for such a small peptide to be evolved into a protein with catalytic functions. On the other hand, the bioinformatics analysis of ZMO1083, ZMO1084 and ZMO1085 in ZM4 identified a putative operon comprising of cellulose synthase catalytic subunits A, B and C (BcsA, BcsB, and BcsC) for cellulose biosynthesis (Asraf, Rajnish, & Gunasekaran, 2011), which show high homology to the cellulose synthesis operon in *Gluconacetobacter xylinus* with the genome loci of H845\_RS02190, H845\_RS02195 and H845\_RS02200 for catalytic subunits (Kubiak et al., 2014).

ZMO1083 encodes BcsA of cellulose synthases, which composes of a UDP-forming subunit and a C-terminal PilZ domain, catalyzing cellulose synthesis from UDP-glucose upon binding to the second messenger bis-(3',5')-cyclic guanosine monophosphate (c-di-GMP) for signal transduction (Asraf et al., 2011; Jeon et al., 2012; Morgan, McNamar, & Zimmer, 2015). The mutation of ZMO1082 in ZM401 disrupted the stop codon TGA for the translation of the putative gene to be terminated as that in ZM4, but continued instead till encountering the stop codon of the neighboring downstream gene ZMO1083. With Open Reading Frame Finder (<https://www.ncbi.nlm.nih.gov/orffinder/>), we predicted that the disrupted ZMO1082 in ZM401 was integrated into ZMO1083 to create a new gene *bcsA\_401* (Figure 5b), since an overlap of 23 nucleotides was detected for the two genes. *bcsA\_401* is larger than ZMO1083, and with TMHMM (<http://www.cbs.dtu.dk/services/TMHMM/>), we predicted that *BcsA\_401* encoded by this gene in ZM401 is a protein bearing eight trans-membrane helices, while the native BcsA in ZM4 was predicted with only six trans-membrane helices (Figure 5c). We compared this analysis with the sequences of amino acid residues and membrane arrangements of the proteins in other cellulose-producing bacteria reported in the NCBI database, and significant homology was observed (date not shown).

Since cellulose synthases are cytoplasmic proteins and cellulose synthesis is a membrane-associated process (Mcnamara, Morgan, & Zimmer, 2015; Morgan, Strumillo, & Zimmer, 2013), we predicted

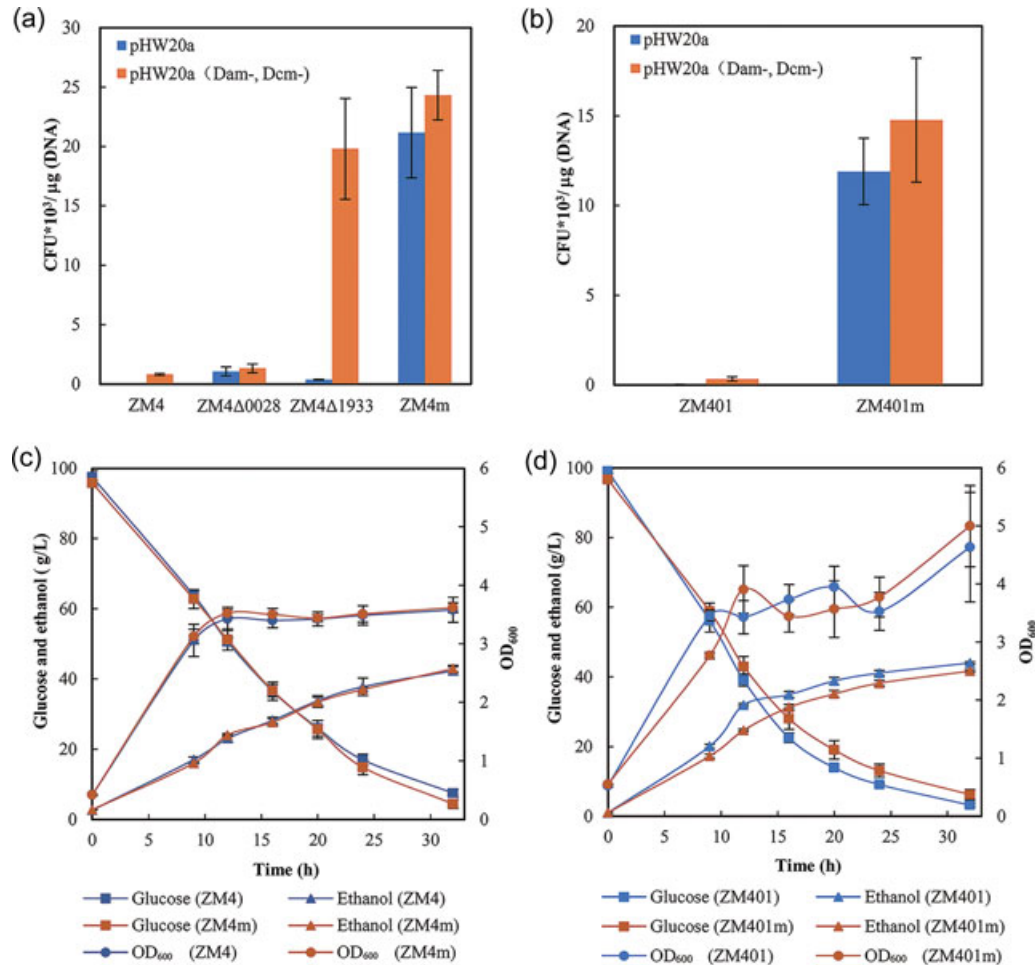


**FIGURE 4** Impact of the deactivation of Type I and Type IV R-M systems in ZM4 (a) and ZM401 (b) on their transformation efficiencies, and ethanol fermentation by both the R-M systems de-activated mutants ZM4 (c) and ZM401 (d) [Color figure can be viewed at [wileyonlinelibrary.com](http://wileyonlinelibrary.com)]

that the difference in the trans-membrane helices would affect their catalytic activities for cellulose biosynthesis and export of synthesized cellulose molecules. Based on the information of *Z. mobilis* in the KEGG database (<http://www.genome.jp/kegg/>), ZMO1086 encodes a glycoside hydrolase for hydrolyzing  $\beta$ -1,4-glucosidic bond in cellulose, which might work similar to another cellulose synthase subunit BcsZ, and act synergistically with BcsA\_ZM4/BcsA\_401 to regulate cellulose synthesis and degradation (Mazur & Zimmer, 2011). Although the mutation in ZMO1082 did not alter the reading of their codons, the expression of *bcsA\_401* in ZM401 and altered configurations and functions with BcsA\_401 might affect the transcription of its neighboring downstream genes *bcsB* and *bcsC* as well as the functions of the proteins they encode. Such a speculation was confirmed by the RT-qPCR analysis, since the upregulation of eight and six folds was observed respectively for the expression of *bcsB* and *bcsC* in ZM401, compared to that detected in ZM4. In the meantime, more significant difference in the transcription of *bcsA\_401* (12-fold upregulation) was also observed in ZM401 compared to that observed with the native *bcsA* in ZM4. The enhanced transcription of the *bcs* operon in ZM401 would benefit its

cellulose synthesis, development of cellulose fibrils and their entanglement for the self-flocculating phenotype of ZM401, which are illustrated schematically in Figure 5d.

The genome sequence comparison did not detect any mutations in genes related to the synthesis of flagella proteins, which not only supported our speculation on their role in the self-flocculation of ZM401, and but also indicates that in-depth studies of molecular mechanism underlying this phenotype should be focused on cellulose biosynthesis, export, and development of cellulose fibrils as well as how these processes are finely regulated for the self-flocculation of the bacterial cells.

### 3.4 | Role of *bcsA\_401* in the self-flocculation of ZM401

To identify the role of *bcsA\_401* in the self-flocculation of ZM401, the knockout of ZMO1083, the major part of *bcsA\_401*, was performed. As expected, the mutant ZM401Δ*bcsA* lost the self-flocculating phenotype, and its flocculating efficiency was almost same as that detected with ZM4, which was in accordance with the very weak

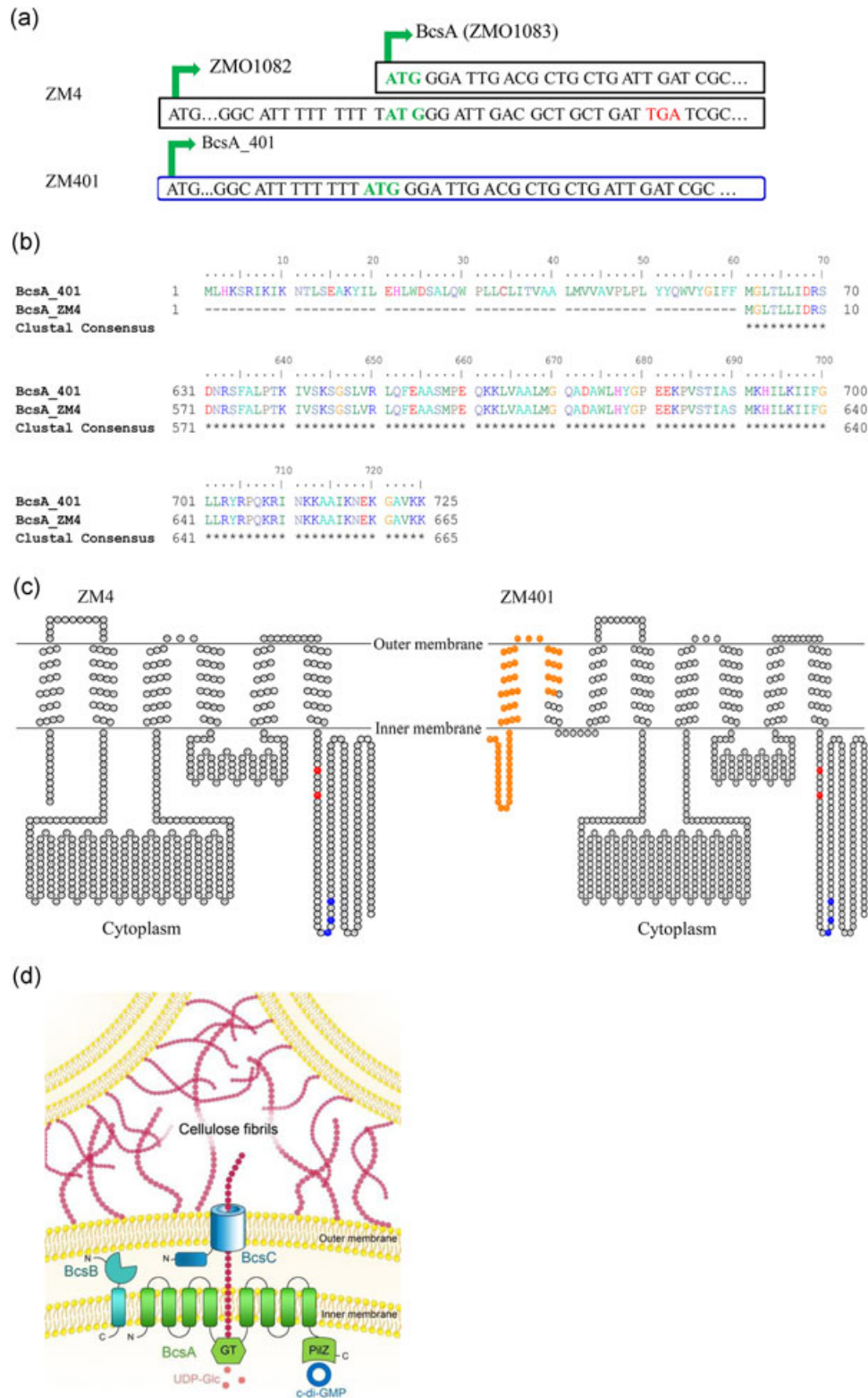


**FIGURE 5** Predicted genes related to cellulose synthesis in ZM4 and ZM401 (a), alignments of the amino acid sequences of the proteins BcsA\_ZM4 and BcsA\_401 (b), their topological models analyzed by TMHMM and illustrated by TOPO2 ([www.sacs.ucsf.edu/cgi-bin/open-topo2.py](http://www.sacs.ucsf.edu/cgi-bin/open-topo2.py)), in which the extra N-terminal and essential sites RxxxR and NxSxxG for c-di-GMP binding are highlighted by orange, red and blue colors, respectively (c), and schematic diagram for the biosynthesis of cellulose fibrils in ZM401 (d). BcsA, BcsB, and BcsC: major cellulose synthase operon proteins. GT: Glucosyltransferase; PilZ: c-di-GMP binding domain in the C-terminal; UDP-Glc: UDP-glucose [Color figure can be viewed at [wileyonlinelibrary.com](http://wileyonlinelibrary.com)]

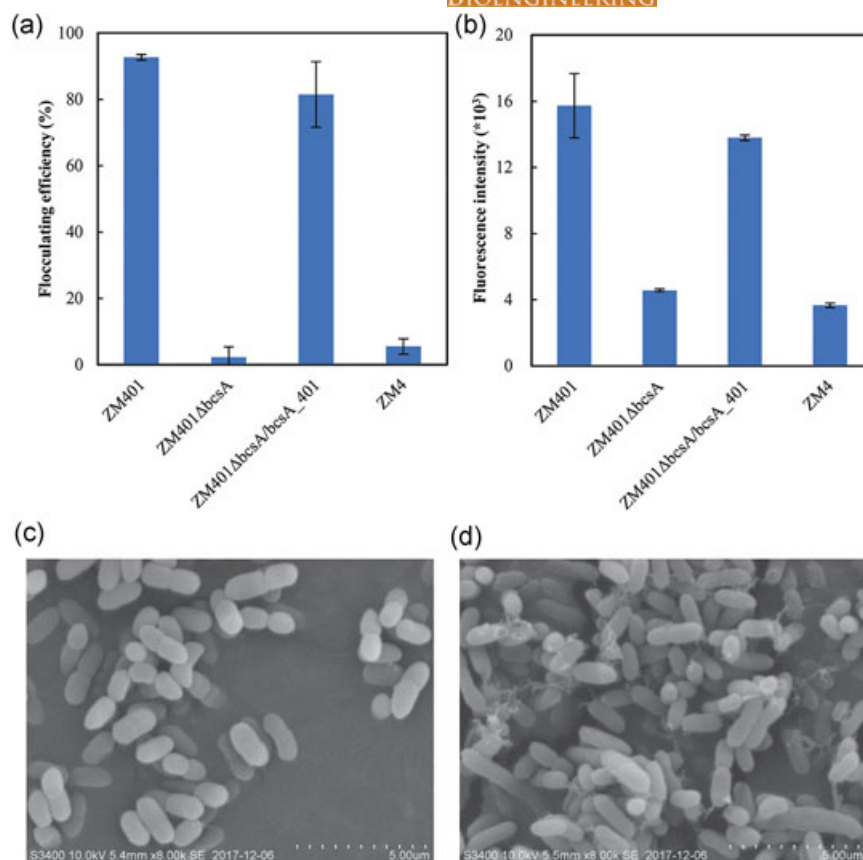


**FIGURE 6** Role of *bcsA\_401* in the self-flocculation of ZM401. Flocculating efficiency (a), fluorescence intensities detected under the Calcofluor-white staining conditions (b), and SEM images of the cell surfaces of ZM401Δ*bcsA* (c) and the complemented mutants of ZM401Δ*bcsA* (d) [Color figure can be viewed at [wileyonlinelibrary.com](http://wileyonlinelibrary.com)]

fluorescence intensity detected under the Calcofluor-white staining conditions (Figure 6a,b). SEM images showed that the cell surfaces of ZM401Δ*bcsA* were smooth without cellulose fibrils (Figure 6c) as that observed in ZM401 previously. These results indicated that the deletion of *bcsA\_401* made the mutant lost the ability for synthesizing cellulose to flocculate the bacterial cells.

We further performed the gene complementation on ZM401Δ*bcsA* under the direction of the native pyruvate decarboxylase promoter (*Ppdc*) from *Z. mobilis* (Conway, Sewell, & Ingram, 1987). No flocculating transformants were selected when *bcsA\_ZM4* was complemented into ZM401Δ*bcsA*. However, when the whole *bcsA\_401* complementation was performed, ZM401Δ*bcsA* restored the self-flocculating phenotype (Figure 6a, b). Morphological observation of the complemented bacterial cells with SEM and cellulase treatment indicated and validated that the self-flocculation was due to the biosynthesis of cellulose, development of cellulose fibrils and their entanglement (Figure 6c,d).

Analysis of BcsA\_401 showed a conserved PilZ domain in the C-terminal characterized by RxxxR and NxSxxG (Figure 5c), which is the binding site for c-di-GMP (Amikam & Galperin, 2006; Benach et al., 2007). As a second messenger, c-di-GMP regulates multiple cellular functions for development and morphogenesis, in particular the synthesis of EPSs in bacteria for biofilm formation (Hengge, 2009; Jenal, Reinders, & Lori, 2017). The PilZ domain of the *G. xylinus* cellulose synthase BcsA binds with c-di-GMP, which acts as an allosteric activator of the cellulose synthase, causing changes in the

configuration and conformation of the enzyme molecule, and consequently initiates cellulose synthesis (Morgan et al., 2015). To explore the role of the PilZ domain in BcsA\_401, we constructed an expression plasmid pHW20a::*bcsA\_401*<sup>R575A</sup> with an alanine residue to substitute the 575th arginine (AxxxR), and introduced the plasmid into ZM401Δ*bcsA* for the gene complementation. Unlike the strain complemented with the native *bcsA\_401*, such a mutant could not restore the self-flocculating phenotype of ZM401. These results indicated the importance of the PilZ domain for cellulose synthase to be functional properly in cellulose biosynthesis. As a result, we deduce that the intracellular level of c-di-GMP would influence the expression of cellulose synthase and its role in cellulose biosynthesis for the self-flocculation of *Z. mobilis*, which should be investigated in the future.

Based on the role of *bcsA\_401* in the self-flocculation of ZM401, we engineered ZM4 with the overexpression of this gene, but unfortunately engineered strains showed very weak self-flocculation with their flocculating efficiencies about 35% only. Take into consideration of the *bcs* operon usually function together, we further overexpressed the whole cellulose synthase operon *bcsABC* from the genome of ZM401 into ZM4. Although the flocculating efficiency was increased to 72%, the self-flocculation was still not complete as that observed in ZM401. Due to the difference in the genome and transcriptome profiles between ZM4 and ZM401, other mechanism needs to be explored for engineering ZM4 and other bacterial cells with desired self-flocculating phenotypes for applications in bioprocess engineering such as the self-immobilization of bacterial cells within bioreactors for high product

productivities as well as merits in microbial physiology associated with the morphological change, particularly the improvement in stress tolerance for high product titers and other benefits.

## 4 | CONCLUSIONS

We confirmed that cellulose synthesized by ZM401 is the major EPS contributing to its self-flocculation. Comparative genome analysis detected the deletion of a nucleotide thymine in ZMO1082, creating a frame-shift mutation and a new gene *bcsA\_401* through integrating ZMO1082 into ZMO1083. We predict that the gene encodes a protein with more transmembrane helices, and changes in the configuration and conformation of the protein would enhance cellulose synthesis and export, development of cellulose fibrils and their entanglement for the self-flocculation of ZM401.

Deactivation of both Type I and Type IV R-M systems in *Z. mobilis* was developed, which significantly improved transformation efficiencies of genetic modifications on the species. The de-flocculation of ZM401 achieved by knocking out *bcsA\_401* and the restoration of the self-flocculating phenotype to ZM401Δ*bcsA* through the gene complementation experimentally supported our speculation on the role of *bcsA\_401* in the self-flocculation of ZM401. The over-expression of *bcsABC\_401* in ZM4 created the self-flocculating phenotype further confirmed the essential role of enhanced cellulose synthesis in the self-flocculation of *Z. mobilis*. The progress will lay a foundation for fundamental research in further deciphering molecular mechanism underlying the self-flocculation of *Z. mobilis* and stress tolerance improvement associated with the morphological change as well as for technological innovations in engineering non-flocculating *Z. mobilis* and other bacterial cells with the self-flocculating phenotype.

## ACKNOWLEDGMENTS

Funding support from the National Science Foundation of China (NSFC) with the grant reference number of (21536006) is acknowledged. The assistance in the EPS analysis and characterization from Professors Guo-Ping Sheng and Yang Mu at the University of Science and Technology of China, and donation of plasmids by Professors Jie Bao at East China University of Science and Technology, Shihui Yang at Hubei University and Ningyi Zhou at Shanghai Jiao Tong University are highly appreciated.

## CONFLICTS OF INTEREST

The authors declare that they have no conflicts of interest.

## AUTHOR CONTRIBUTIONS

J. Xia designed a roadmap for this study under the supervision of F.-W. Bia, completed all experiments, interpreted data and developed

a manuscript draft. C.-G. Liu supervised the culture and ethanol fermentation of *Z. mobilis*. X.-Q. Zhao supervised molecular manipulations on *Z. mobilis*; Y. Xiao and X.-X. Xia critically commented on this manuscript. F.-W. Bia supervised the whole research, analyzed the data and other results with all co-authors and rewrote this manuscript.

## ORCID

Feng-Wu Bai  <http://orcid.org/0000-0003-1431-4839>

## REFERENCES

- Amikam, D., & Galperin, M. Y. (2006). PilZ domain is part of the bacterial c-di-GMP binding protein. *Bioinformatics*, 22(1), 3–6.
- Asraf, S. A. K. S., Rajnish, K. N., & Gunasekaran, P. (2011). Bioinformatics and biosynthesis analysis of cellulose synthase operon in *Zymomonas mobilis* ZM4. *The IIOAB Journal*, 2(3), 1–7.
- Bai, F. W., Anderson, W. A., & Moo-Young, M. (2008). Ethanol fermentation technologies from sugar and starch feedstocks. *Biotechnology Advances*, 26, 89–105.
- Benach, J., Swaminathan, S. S., Tamayo, R., Handelman, S. K., Folta-Stogniew, E., Ramos, J. E., ... Hunt, J. F. (2007). The structural basis of cyclic diguanylate signal transduction by PilZ domains. *The EMBO Journal*, 26, 5153–5166.
- Chong, S., Sen, T. K., Kayaalp, A., & Ang, H. M. (2012). The performance enhancements of upflow anaerobic sludge blanket (UASB) reactors for domestic sludge treatment – A state-of-the-art review. *Water Research*, 46, 3434–3470.
- Conway, T., Sewell, G. W., & Ingram, L. O. (1987). Glyceraldehyde-3-phosphate dehydrogenase gene from *Zymomonas mobilis*: Cloning, sequencing, and identification of promoter region. *Journal of Bacteriology*, 169, 5653–5662.
- Cowles, K. N., Willis, D. K., Engel, T. N., Jones, J. B., & Barak, J. D. (2015). Diguanylate cyclases AdrA and STM1987 regulate *Salmonella enterica* exopolysaccharide production during plant colonization in an environment-dependent manner. *Applied and Environmental Microbiology*, 82, 1237–1248.
- Dong, H. W., Bao, J., Ryu, D. D. Y., & Zhong, J. J. (2011). Design and construction of improved new vectors for *Zymomonas mobilis* recombinants. *Biotechnology and Bioengineering*, 108, 1616–1627.
- Flemming, H. C., & Wingender, J. (2010). The biofilm matrix. *Natural Reviews Microbiology*, 8, 623–633.
- Flemming, H. C., Wingender, J., Szewzyk, U., Steinberg, P., Rice, S. A., & Kjelleberg, S. (2016). Biofilms: An emergent form of bacterial life. *Natural Reviews Microbiology*, 14, 563–575.
- Gu, H., Zhang, J., & Bao, J. (2015). High tolerance and physiological mechanism of *Zymomonas mobilis* to phenolic inhibitors in ethanol fermentation of corncob residue. *Biotechnology and Bioengineering*, 112, 1770–1782.
- Halme, A., Bumgarner, S., Styles, C., & Fink, G. R. (2004). Genetic and epigenetic regulation of the *FLO* gene family generates cell-surface variation in yeast. *Cell*, 116, 405–415.
- He, L. Y., Zhao, X. Q., & Bai, F. W. (2012). Engineering industrial *Saccharomyces cerevisiae* strain with the *FLO1*-derivative gene isolated from the flocculating yeast SPSC01 for constitutive flocculation and fuel ethanol production. *Applied Energy*, 100, 33–40.
- He, M., Wu, B., Qin, H., Ruan, Z., Tan, F., Wang, J., ... Hu, Q. (2014). *Zymomonas mobilis*: A novel platform for future biorefineries. *Biotechnology for Biofuels*, 7, 101.
- Hengge, R. (2009). Principles of c-di-GMP signaling in bacteria. *Natural Reviews Microbiology*, 7, 263–273.

- Hmelo, L. R., Borlee, B. R., Almlad, H., Love, M. E., Randall, T. E., Tseng, B. S., ... Harrison, J. J. (2015). Precision-engineering the *Pseudomonas aeruginosa* genome with two-step allelic exchange. *Natural Protocols*, 10, 1820–1841.
- Hoang, T. T., Karkhoff-Schweizer, R. R., Kutchma, A. J., Schweizer, H. P. (1998). A broad-host-range Flp-FRT recombination system for site-specific excision of chromosomally-located DNA sequences: application for isolation of unmarked *Pseudomonas aeruginosa* mutants.
- Jeffries, T. W. (2006). Engineering yeasts for xylose metabolism. *Current Opinion in Biotechnology*, 17, 320–326.
- Jenal, U., Reinders, A., & Lori, C. (2017). Cyclic di-G-MP: Second messenger extraordinaire. *Natural Reviews Microbiology*, 15, 271–284.
- Jeon, Y. J., Xun, Z., Su, P., & Rogers, P. L. (2012). Genome-wide transcriptomic analysis of a flocculent strain of *Zymomonas mobilis*. *Applied Microbiology and Biotechnology*, 93, 2513–2518.
- Ju, F., & Zhang, T. (2015). Bacterial assembly and temporal dynamics in activated sludge of a full-scale municipal wastewater treatment plant. *The ISME Journal*, 9, 683–695.
- Kalnenieks, U. (2006). Physiology of *Zymomonas mobilis*: Some unanswered questions. *Advances in Microbial Physiology*, 51, 73–117.
- Kerr, A. L., Jeon, Y. J., Svenson, C. J., Rogers, P. L., & Neilan, B. A. (2011). DNA restriction-modification systems in the ethanologen *Zymomonas mobilis* ZM4. *Applied Microbiology and Biotechnology*, 89, 761–769.
- Kubiak, K., Kurzawa, M., Jędrzejczak-Krzepkowska, M., Ludwicka, K., Krawczyk, M., Migdalski, A., ... Bielecki, S. (2014). Complete genome sequence of *Gluconacetobacter xylinus* E25 strain-valuable and effective producer of bacterial nanocellulose. *Journal of Biotechnology*, 176, 18–19.
- Li, Q., Zhao, X. Q., Chang, A. K., Zhang, Q. M., & Bai, F. W. (2012). Ethanol-induced yeast flocculation directed by the promoter of *TPS1* encoding trehalose-6-phosphate synthase 1 for efficient ethanol production. *Metabolic Engineering*, 14, 1–8.
- Li, X., Thomason, L. C., Sawitzke, J. A., Costantino, N., & Court, D. L. (2013). Positive and negative selection using the *tetA-sacB* cassette: Recombineering and P1 transduction in *Escherichia coli*. *Nucleic Acids Research*, 41(22), e204–e204.
- Lim, S. J., & Kim, T. H. (2014). Applicability and trends of anaerobic granular sludge treatment processes. *Biomass and Bioenergy*, 60, 189–202.
- Limoli, D. H., Jones, C. J., & Wozniak, D. J. (2015). Bacterial extracellular polysaccharides in biofilm formation and function. *Microbiol Spectrum*, 3(3), MB-0011-2014. <https://doi.org/10.1128/microbiolspec.MB-0011-2014>
- Liu, X. M., Sheng, G. P., Luo, H. W., Zhang, F., Yuan, S. J., Xu, J., ... Yu, H. Q. (2010). Contribution of extracellular polymeric substances (EPS) to the sludge aggregation. *Environmental Science and Technology*, 44, 4355–4360.
- Mazur, O., & Zimmer, J. (2011). Apo- and cellopentaose-bound structures of the bacterial cellulose synthase subunit BcsZ. *Journal of Biological Chemistry*, 286, 17601–17606.
- Mcnamara, J. T., Morgan, J. L. W., & Zimmer, J. (2015). A molecular description of cellulose biosynthesis. *Annual Review of Biochemistry*, 84, 895–921.
- Morgan, J. L. W., McNamar, J. T., & Zimmer, J. (2015). Mechanism of activation of bacterial cellulose synthase by cyclic di-GMP. *Nature Structural & Molecular Biology*, 21, 489–496.
- Morgan, J. L. W., Strumillo, J., & Zimmer, J. (2013). Crystallographic snapshot of cellulose synthesis and membrane translocation. *Nature*, 493, 181–186.
- Palha, M. A. P. F., Lopes, C. E., & Pereira, N., jr. (1997). Ethanol stimulates the flocculation of *Zymomonas mobilis*. *Biotechnology Letters*, 19, 499–501.
- Papenfort, K., & Bassler, B. L. (2016). Quorum sensing signal-response systems in Gram-negative bacteria. *Natural Reviews Microbiology*, 14, 576–588.
- Seo, J. S., Chong, H., Park, H. S., Yoon, K. O., Jung, C., Kim, J. J., ... Kang, H. S. (2005). The genome sequence of the ethanologenic bacterium *Zymomonas mobilis* ZM4. *Nature Biotechnology*, 23, 63–68.
- Serra, D. O., Richter, A. M., & Hengge, R. (2013). Cellulose as an architectural element in spatially structured *Escherichia coli* biofilms. *Journal of Bacteriology*, 195, 5540–5554.
- Soares, E. V. (2010). Flocculation in *Saccharomyces cerevisiae*: A review. *Journal of Applied Microbiology*, 110, 1–18.
- Verstrepen, K. J., Jansen, A., Lewitter, F., & Fink, G. R. (2005). Intragenic tandem repeats generate functional variability. *Nature Genetics*, 37, 986–990.
- Xue, C., Zhao, X. Q., & Bai, F. W. (2010). Effect of the size of yeast flocs and zinc supplementation on continuous ethanol fermentation performance and metabolic flux distributions under very high concentration conditions. *Biotechnology and Bioengineering*, 105, 935–944.
- Yang, S., Mohagheghi, A., Franden, M. A., Chou, Y. C., Chen, X., Dowe, N., ... Zhang, M. (2016). Metabolic engineering of *Zymomonas mobilis* for 2,3-butanediol production from lignocellulosic biomass sugars. *Biotechnology for Biofuels*, 9, 189.
- Yang, S., Pappas, K. M., Hauser, L. J., Land, M. L., Chen, G. L., Hurst, G. B., ... Brown, S. D. (2009). Improved genome annotation for *Zymomonas mobilis*. *Nature Biotechnology*, 27(10), 893–894.
- Yang, S., Fei, Q., Zhang, Y. P., Contreras, L. M., Utturkar, S. M., Brawn, S. D., & Zhang, M. (2016). *Zymomonas mobilis* as a model system for production of biofuels and biochemical. *Microbial Biotechnology*, 9, 699–717.
- Zhang, K., Shao, H., Cao, Q., He, M., Wu, B., & Feng, H. (2015). Transcriptional analysis of adaptation to high glucose concentrations in *Zymomonas mobilis*. *Applied Microbiology and Biotechnology*, 99, 2009–2022.
- Zhang, M., Eddy, C., Deanda, K., Finkelstein, M., & Picataggio, S. (1995). Metabolic engineering of a pentose metabolism pathway in ethanologenic *Zymomonas mobilis*. *Science*, 267, 240–243.
- Zhao, N., Bai, Y., Liu, C. G., Zhao, X. Q., Xu, J. F., & Bai, F. W. (2014). Flocculating *Zymomonas mobilis* is a promising host to be engineered for fuel ethanol production from lignocellulosic biomass. *Biotechnology Journal*, 9, 362–371.
- Zhao, N., Bai, Y., Zhao, X. Q., Yang, Z. Y., & Bai, F. W. (2012). Draft genome sequence of the flocculating *Zymomonas mobilis* strain ZM401 (ATCC 31822). *Journal of Bacteriology*, 194, 7008–7009.
- Zhao, X. Q., & Bai, F. W. (2009). Yeast flocculation: New story in fuel ethanol production. *Biotechnology Advances*, 27, 849–856.

**How to cite this article:** Xia J, Liu C-G, Zhao X-Q, Xiao Y, Xia X-X, Bai F-W. Contribution of cellulose synthesis, formation of fibrils and their entanglement to the self-flocculation of *Zymomonas mobilis*. *Biotechnology and Bioengineering*. 2018;115:2714–2725. <https://doi.org/10.1002/bit.26806>